

DEPENDENCE OF THE EFFICIENCY OF EXCIMER GAS-DISCHARGE LASERS ON PARAMETERS OF THE EXCITATION CIRCUIT AND THE ACTIVE MEDIUM

A.M. RAZHEV, A.A. ZHUPIKOV, A.G. KALYUZHNYAYA¹, A.I. SHCHEDRIN¹

UDC 532.621
© 2005

Institute of Laser Physics, Acad. Sci. of Russia, Siberia Division
(13/3, Lavrent'yeva Prosp., Novosibirsk 630090, Russia),

¹Institute of Physics, Nat. Acad. Sci. of Ukraine
(46, Nauky Prosp., Kyiv 03028, Ukraine)

We present the theoretical and experimental results of studies of the influence of parameters of the excitation system and the active medium on the radiant energy and efficiency of a KrF laser. An *LC*-inverter excitation circuit with a sharpening capacitor, the automatic UV preionization, and a spark gap used as a high-voltage switch is analyzed. The optimal parameters of elements of the excitation circuit are found, which provides the pumping intensity approximately equal to 4 MW/cm³. It is discovered that the increase in the pumping level yields a rise of both the total pressure of the active medium and the active volume due to an increase of the discharge width. A comparison of the results obtained for KrF and ArF lasers testifies to the fact that the dependences of the discharge and radiation characteristics on the parameters of the excitation circuit have a universal form.

1. Introduction

For the majority of practical applications, the most important parameters of an excimer laser are the maximum pulse energy of radiation attainable at the highest possible efficiency with respect to the stored energy, reliability and effectiveness of the electric circuit used for laser excitation, as well as the cost of its exploitation which is mainly determined by the cost of a gas mixture. It is known that the usage of helium as a buffer gas instead of neon allows one to decrease essentially the cost of laser operation. That's why, the development of a powerful high-performance laser with an active medium based on a buffer gas helium represents an urgent problem.

In our opinion, the most important parameter responsible for the achievement of high values of the laser radiant energy and efficiency is a pumping intensity. In the present paper, by a pumping intensity, we mean the power density W of the pumping of an active medium, which is determined as $W = E/V\tau$, where E is the energy stored in a sharpening capacitor, V — the active volume, τ — the duration of the first half-

period of the discharge current measured on the base level.

In [1], it was shown that the achievement of high values of the radiant energy and efficiency of a neon-based KrF laser requires a pumping intensity in the range 1.8–2.5 MW/cm³. At such a pumping intensity, a laser excited by means of a capacitor recharge circuit with automatic UV preionization provides the radiant energy of 500 mJ at the total efficiency of 3.9%. In [2], a laser analogous to that described in [1] emitted the radiant energy of 810 mJ at the efficiency of 2.6%.

In [3], the excitation system analogous to that used in [1, 2] allowed one to achieve the radiant energy of 600 mJ and the efficiency of 1.6% at a charging voltage of 36 kV, while the highest possible value of the efficiency equal to 2.8% was obtained at the energy of 300 mJ. In this case, the estimated pumping intensity approximated 2.0 MW/cm³.

Paper [4] was devoted to investigating a He–Kr–F₂ mixture laser. It was excited with the help of a pumping system similar to that described in [1, 2]. The radiant energy obtained in these researches at the charging voltage of 45 kV and the active volume of 200 cm³ amounted to 500 mJ, while the efficiency was equal to 1.1%.

The maximal energy of a gas discharge KrF laser was obtained in [5] and amounted to 5 J in a neon-based laser and 4.5 J in a helium one. In order to attain so high energies, a complicated pumping system was developed according to a two-stage Marx generator circuit that operated at charging voltages of 190–220 kV. The efficiency of such a KrF laser calculated with respect to the energy stored in capacitors did not exceed 0.53 and 0.47%, respectively.

In [6], the same authors replaced a Marx generator by an *LC*-inverter excitation system with magnetic contraction links used for exciting the active volume

$6.5 \times 5.0 \times 80 \text{ cm}^3$, which allowed them to reduce the charging voltage from 192 to 65 kV. In this case, the radiant energy in a Ne–Kr–F₂ mixture medium decreased from 5.0 to 2.5 J, while the total efficiency increased up to 2.5%. Under these conditions, the pumping intensity was equal to 0.6 MW/cm^3 . However, the usage of helium as a buffer gas at such low pumping intensity did not allow the authors to obtain high values of the radiant energy and efficiency of the KrF laser, and they did not report any information about the latter.

In order to obtain the effective generation of a He–Kr–F₂ mixture laser, we increased the pumping intensity up to 3.0 MW/cm^3 , which allowed us to create such a laser with a radiant energy of 800 mJ and a total efficiency of 2.0% [7].

As follows from the above literature review, the highest values of the radiant energy and efficiency of a KrF laser were obtained with the mixture Ne–Kr–F₂ at the pumping intensity of 2.0 MW/cm^3 . A replacement of the buffer gas helium by neon required an increase of the pumping intensity up to 3 MW/cm^3 and higher.

The purpose of the present paper consists in the theoretical and experimental investigation of the processes taking place in the excitation system and the active medium of a He–Kr–F₂ mixture laser in order to achieve the highest possible values of its radiant energy and efficiency. The problem also includes the search for the optimal values of the active medium configuration and the elements of the high-voltage excitation system, as well as the determination of the optimal parameters of the excitation of a He–Kr–F₂ mixture laser.

2. Experimental Setup

The experimental investigations consisted in measuring the energy and amplitude-time characteristics of voltage, current, and radiation pulses in the nanosecond interval. The apparatus and measuring techniques are described in [8].

The distance between the basic electrodes in the discharge chamber was equal to 2.7 cm. The length of the active part amounted to 59 cm, while the discharge width represented a variable quantity depending on pumping parameters and was determined by the light spot. The minimal discharge width equal to 0.7 cm was obtained at a charging voltage of 18 kV and increased up to 1.1 cm with increase in a charging voltage up to 26 kV. Thus, the active volume varied from 96 to 175 cm³ depending on the pumping level. The automatic UV preionization was performed by two rows of spark gaps located astride one of the basic electrodes. The discharge

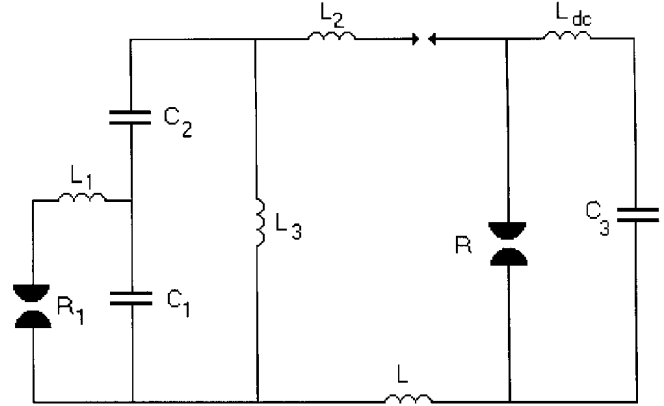


Fig. 1. *LC*-inverter electric circuit used for laser pumping: $C_1 = 50 \text{ nF}$, $C_2 = 100 \text{ nF}$, $C_3 = 30 \text{ nF}$, $R_1 = 0.1 \div 0.15 \Omega$, $L_1 = 40 \div 70 \text{ nH}$, $L_2 = 13 \text{ nH}$, $L_3 = 2.5 \mu\text{H}$, $L_{dc} = 3.8 \text{ nH}$

chamber was sealed by means of parallel-sided plates made of MgF₂, one of which served as an exit mirror of the resonator. Its second mirror was an external dielectric mirror with a reflection coefficient of 99% at a radiation wavelength of 248 nm. The optical length of the resonator amounted to 120 cm.

As an excitation system, we used an *LC*-inverter circuit with a sharpening capacitor and automatic preionization. Such a choice was conditioned by a number of advantages of this circuit as compared to that of the *C–C* recharge type. First, it's worth noting the possibility to reach high voltages across a discharge gap, which contributes to both the improvement of the discharge homogeneity and an increase in the efficiency of energy transmission to an active medium at low charging voltages. Secondly, a high-voltage switch is not introduced into a circuit in series and therefore transmits only a part of the stored energy, which ensures both a decrease in the load on a high-voltage switch and an increase in its service life.

An *LC* inverter, first proposed for pumping excimer lasers in [9], represents a pulse generator with the voltage doubling due to its inversion across one of reservoir capacitors (Fig. 1). The reservoir capacitors C_1 and C_2 are charged from a source up to a charging voltage U_C . The operation of a gas-filled gap R_1 causes an oscillation process arising in the L_1C_1 circuit, which results in recharging of C_1 after the time interval $\pi\sqrt{L_1C_1}$, so that the voltage U across C_3 exceeds the charging one. By that moment, the capacitor C_2 turns out to be discharged to a certain extent. In order to minimize the influence of this factor, the value of the capacity

C_2 is chosen to be higher than C_1 (usually $C_2 \approx 2C_1$).

The sharpening capacity C_3 represents a capacitor connected in parallel to a discharge gap. It is used for creating a low-inductance circuit with the latter, i.e. for time “sharpening” of the discharge current passing through the gap with respect to the current charging C_3 . The magnitude of the capacity C_3 is chosen on the ground of providing the most efficient energy transfer from the reservoir capacitors to the sharpening one. One can demonstrate that this requirement is satisfied under the condition that $C_3 \approx (1/C_1 + 1/C_2)^{-1}$.

The inductance L_2 includes that of UV preionization and those of the capacitors C_1 and C_2 , L_1 stands for the inductance of the L_1C_1 circuit (which is mostly determined by that of the gas-filled gap R_1), and L_3 is the charging inductance. L denotes the inductance of buses supplying current. Creators of excimer lasers usually aim at the value of L equal to 20–30 nH. The discharge itself represents an ohmic time-dependent resistance which is determined by the density of electrons and their mobility in the discharge. L_{dc} is the inductance of the discharge circuit, whose magnitude lies in the range 3–5 nH.

As a high-voltage switch, we used two kinds of spark gaps — a standard RU-65 gas-filled gap ($R_1 \sim 0.15 \Omega$, $L_1 \sim 70$ nH) and a specially developed one (SR) characterized with lower values of resistance and self-inductance ($R_1 \sim 0.1 \Omega$, $L_1 \sim 40$ nH).

3. The Theoretical Model

The discharge and radiation dynamics was numerically simulated by means of solving the kinetic equations for components of the mixture together with the equation for the feed circuit and the Boltzmann equation for the electron energy distribution function in an electric field:

$$\frac{1}{n_e N} \sqrt{\frac{m\varepsilon}{2e}} \frac{\partial(n_e f_0)}{\partial t} - \frac{1}{3} \left(\frac{E}{N}\right)^2 \frac{\partial}{\partial \varepsilon} \left(\frac{\varepsilon}{\sum_i \frac{N_i}{N} Q_{Ti}} \frac{\partial f_0}{\partial \varepsilon} \right) - \frac{\partial}{\partial \varepsilon} \left[2 \sum_i \frac{N_i m}{N M_i} Q_{Ti} \varepsilon^2 \left(f_0 + T \frac{\partial f_0}{\partial \varepsilon} \right) \right] = S_{eN}, \quad (1)$$

where ε stands for the energy of electrons, n_e — their density, E — the electric field, T — the gas temperature (eV), N — the total gas concentration, N_i , M_i , and Q_{iT} denote the concentrations of atoms and molecules, their masses, and transport cross sections, respectively, m — the electron mass, and $e = 1.602 \times 10^{-12}$ erg/eV.

The integral S_{eN} describing inelastic electron collisions with atoms and molecules has a form

$$S_{eN} = \sum_i \frac{N_i}{N} \times \times [(\varepsilon + \varepsilon_i) Q_i(\varepsilon + \varepsilon_i) f_0(\varepsilon + \varepsilon_i) - \varepsilon Q_i(\varepsilon) f_0(\varepsilon)] - \frac{N_{at}}{N} \varepsilon Q_{at}(\varepsilon) f_0(\varepsilon), \quad (2)$$

where Q_i and ε_i denote the cross sections and energy thresholds for the processes of excitation and ionization of inert gas atoms and fluorine molecules, and Q_{at} is the cross section for the electron attachment to fluorine molecules.

The kinetic processes taken into account when numerically simulating the plasma kinetics of a KrF laser are given in [10].

4. Discussion of the Results

In the present work, we analyze theoretically a KrF laser based on the mixture He:Kr:F₂=89.8:10:0.2 at a pressure of 2.5 atm and a charging voltage of 21 kV in order to determine the optimal parameters of the excitation circuit. The results of the theoretical analysis were compared to experimental data. We analyzed the operation of the excitation circuit depending on values of its basic parameters: the inductance L of buses supplying current that influences the effectiveness of energy transfer from the reservoir capacitors to the sharpening one, the resistance of a gas-filled gap R_1 , and its inductance L_1 that determine the efficiency of the operation of the voltage doubling circuit.

The optimal operation of the considered excitation circuit requires an effective voltage doubling across the reservoir capacitors as well as the most complete transmission of the stored energy to the sharpening capacitor and the discharge. In addition, the rate of transmitting the energy to the discharge is also of importance, as it directly influences the homogeneity of the preionization of the working volume. The optimal excitation system of a laser should provide a time delay between the preionization pulse and the discharge breakdown sufficient for preionization electrons to be distributed uniformly inside the volume of the discharge chamber.

The discharge dynamics essentially depends on the magnitude of the inductance L of buses supplying current. Figure 2 shows its influence on the effectiveness η' of the energy transfer from the electric circuit to the

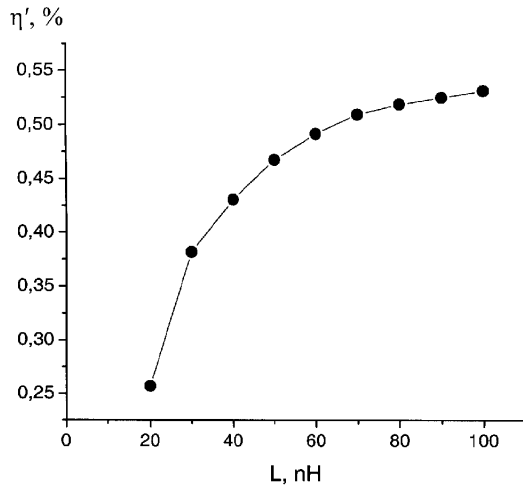
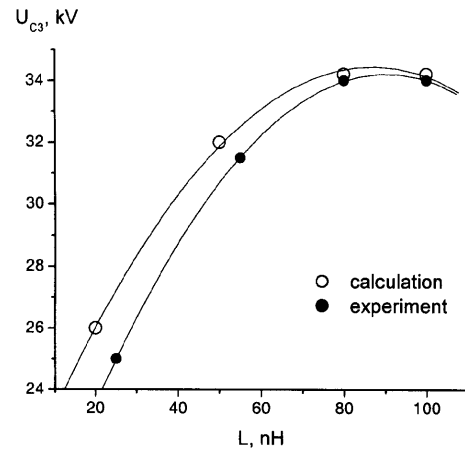


Fig. 2. Effectiveness of the energy transfer to a discharge as a function of the inductance L

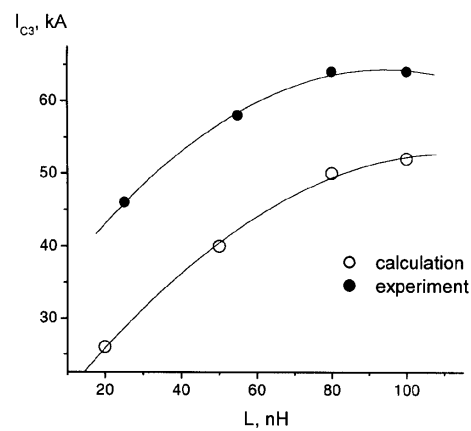
discharge (i.e. the ratio of the energy transmitted to the capacitor C_3 to that stored in the reservoir capacitors C_1 and C_2). In this case, the values of L_1 and R_1 amount to 70 nH and 0.15 Ω , which corresponds to the parameters of a RU-65 gas-filled gap. As follows from our calculations, there exists a range of values of the inductance L , at which the energy is transmitted to the discharge in the optimal mode. At the chosen values of the other parameters, such a mode corresponds to the range of $L \sim 80 \div 100$ nH.

In Fig. 3, *a, b*, we present the experimental and calculated dependences of the voltage across the capacitor C_3 and the current passing through it on the inductance L obtained at a charging voltage of 21 kV. In addition to an increase of the discharge voltage and current, a rise of the inductance L is accompanied with a pulling of the breakdown time moment, i.e. with an increase in the time delay τ between the preionization pulse and that of the discharge current (Fig. 3, *c*). It is natural, as a growth of the inductance of a circuit results in a rise of the period of electric oscillations in it. A later breakdown is advantageous from the viewpoint of the improvement of the preionization homogeneity in a discharge. This effect cannot be reflected in calculations, since the preionization is considered to be uniform in the whole volume of the discharge chamber, but it takes place in practice. As was shown in [11,12], the maximal radiant energy is reached at the time delay equal to 200–300 ns. That's why, the approach to the range of optimal values of τ also causes an increase in the laser energy and efficiency.

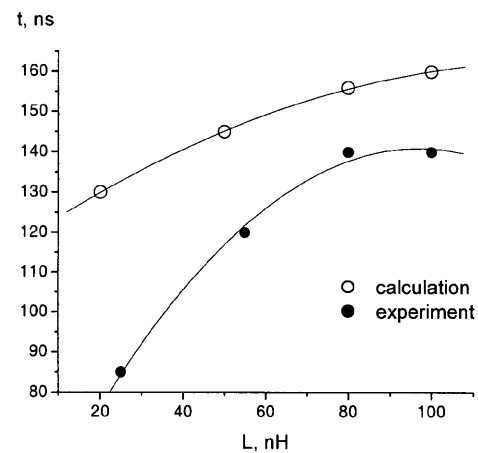
The magnitude of the inductance of the $L_1 C_1$ circuit also exerts an essential influence on the discharge



a



b



c

Fig. 3. Influence of the inductance L on the discharge characteristics: *a* — the voltage across the capacitor C_3 ; *b* — the current passing through C_3 ; *c* — the time delay between the preionization pulse and the discharge breakdown

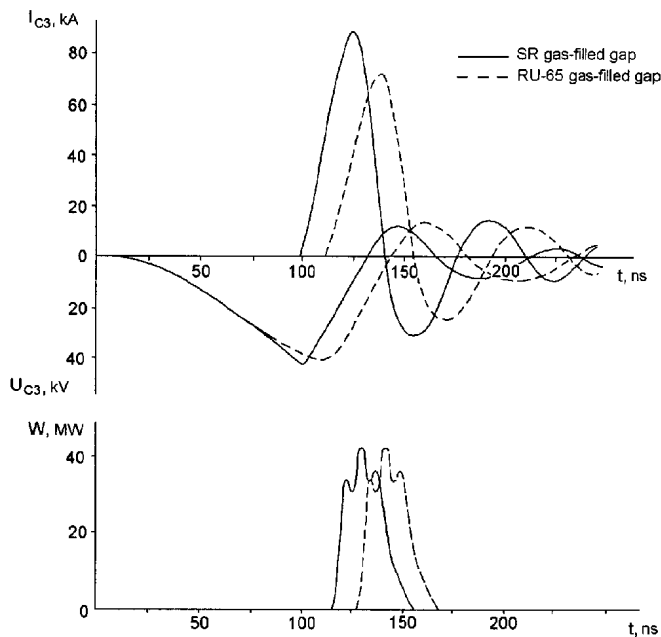


Fig. 4. Experimental oscillograms of the voltage across the capacitor C_3 , the current passing through it, and the radiation power obtained using different gas-filled gaps

dynamics. In Fig. 4, we present the experimental oscillograms of the voltage across the capacitor C_3 , the current passing through it, and the radiation power measured using different gas-filled gaps [a RU-65 ($L_1 = 70$ nH, $R_1 = 0.15 \Omega$) and a specially developed discharger SR ($L_1 = 40$ nH, $R_1 = 0.1 \Omega$) characterized with lower values of the resistance and self-inductance]. One can see that, with decrease in L_1 , the breakdown of the discharge gap takes place earlier, while the ignition potential and the discharge current increase. These facts can be easily explained, since a decrease in the inductance of the $L_1 C_1$ circuit results in a reduction of its oscillation period, i.e. in the earlier achievement of the inversed voltage across the capacitor C_1 and, respectively, the doubled voltage across the condensers C_1, C_2 . Moreover, the voltage doubling takes place with lower losses as, during a shorter time of recharging of C_1 , the capacitor C_2 cannot discharge essentially. As the duration of the stage preceding the initiation of the discharge reduces, the electron density necessary for a breakdown can be obtained only at a higher discharge voltage.

Thus, with decrease in the inductance L_1 , the voltage across the discharge gap rises, which implies a more effective energy transfer to the discharge, but the time delay between the beginning of the preionization pulse and the discharge ignition shortens, which results

in worsening the preionization homogeneity of the working volume. That's why, when choosing the optimal parameters of the excitation system, it is necessary to find a compromise between these two factors. An analysis of the experimental oscillograms (Fig. 4) demonstrates that making use of lower values of the inductance L_1 causes an increase of the discharge current (in this case, the radiant energy rises by 10%) in spite of the fact that the time delay between the preionization pulse and the discharge breakdown reduces by approximately 10 ns.

The resistance of a gas-filled gap R_1 determines the degree of the damping of electric oscillations in the $L_1 C_1$ circuit. If we use the considered excitation circuit with a gas-filled gap with the resistance $R_1 > 0.5 \Omega$, oscillations in the $L_1 C_1$ circuit damp during the first half-period, and the voltage reached across the reservoir capacitors after the recharging of C_1 does not exceed practically the charging one, so that the usage of the voltage doubling circuit makes no sense. A variation of the resistance R_1 in the range of low values ~ 0.1 – 0.2Ω almost does not influence the discharge dynamics, by resulting only in a slight change of the ignition potential.

Thus, choosing the optimal values of the inductance L of buses supplying current and the inductance L_1 , one can transfer the energy to the discharge more effectively, which causes an essential increase of the ignition potential and the discharge current (Fig. 5, *a*). Moreover, the dependences of the discharge voltage and current on the circuit parameters have a universal form for various active media of excimer lasers. In Fig. 5, *b*, we present the voltage across the capacitor C_3 and the current passing through it as functions of the inductances L and L_1 calculated for an ArF laser based on the He:Ar:F₂ mixture excited with the considered LC -inverter circuit. In this case, the mixture components relate as 79.7:20:0.3, the total pressure of the active medium equals 1.6 atm, and the charging voltage amounts to 21 kV [13]. A numerical simulation of the plasma kinetics is performed using the kinetic processes given in [14].

It's worth noting that the calculated radiant energy rather slightly depends on the inductances L and L_1 though, according to the experimental data, a transition to the range of their optimal values results in an increase of the radiant energy by a factor of 1.5–2. In order to describe the influence of the parameters of the feed circuit on the radiant energy of a laser in more details, one should take into account the expansion of the region of discharge burning that takes place as the discharge

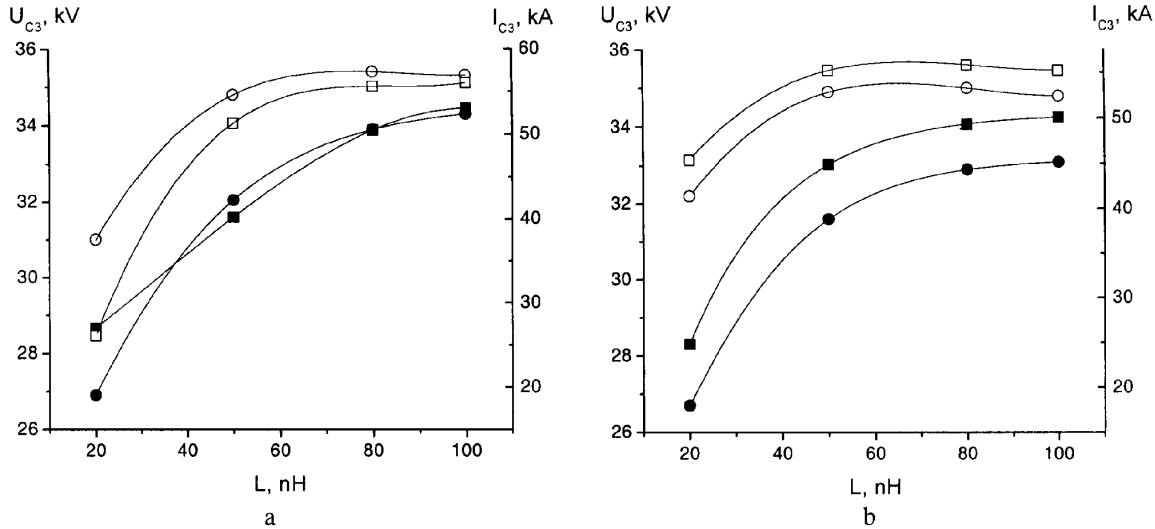


Fig. 5. Dependences of the voltage across the capacitors C_3 (\bullet , \circ) and current passing through it \blacksquare , \square on the inductances L , L_1 calculated for He:Kr:F₂ (a) and He:Ar:F₂ (b) lasers. \bullet , \circ — $L_1=70$ nH, \blacksquare , \square — $L_2=40$ nH

voltage increases. Such an effect is conditioned by the influence of the real profile of electrodes on the space-time dynamics of the discharge (STDD) and radiation. Electrodes used in practice have a special form providing the improvement of the uniformity of the electric field in a discharge. Their surfaces can be approximately represented as parts of a cylinder with a large (as compared to the electrode width) radius of curvature R , so as the distance between the electrodes gradually increases in the direction from their center to the periphery. It is clear that the breakdown in such a system takes place only in the central part of the electrodes. In peripheral layers, the magnitude of the electric field is insufficient for the discharge ignition. A rise of the voltage across the discharge gap and, respectively, the electric field between the electrodes must induce an increase of the number of layers involved in the discharge process, i.e. an expansion of the region of discharge burning.

In order to allow for the influence of the electrode profile on the STDD, we used a model described in [15]: the discharge gap was decomposed into $n + 1$ layers with a small width along the electric field lines. The calculation of STDD consisted in the simulation of the time characteristics of the plasma in each of these layers. The field intensity in the i -th layer depends on the length of the field line l_i : $E_i = U/l_i$, where U is the discharge voltage. The length of the field lines increases from the center towards the periphery of electrodes:

$$l_i = \frac{2\vartheta_i}{\sin \vartheta_i} \left[R(1 - \cos \vartheta_i) + \frac{d}{2} \right], \quad (3)$$

where $\vartheta_i = i \frac{\vartheta_{\max}}{2n+1}$, $\vartheta_{\max} = 2 \arctg \frac{B}{\sqrt{4R^2 - B^2}}$, $i = 0, 1, \dots, n$, d is the distance between the electrodes along the discharge axis, and B is the width of the electrode base.

In Fig. 6, we demonstrate the dependences of the voltage across the capacitor C_3 (a) and the current passing through it (b) on the inductances L and L_1 calculated for the case of plane electrodes and those of cylindrical form with the curvature radius $R=10$ cm. In this case, the width of the electrode base amounts to 3 cm, and the interelectrode distance equals 2.7 cm, which corresponds to the experimental parameters. A comparison of the curves shows that the allowance for the influence of the electrode profile on the STDD has no effect practically on the form of the dependences of the voltage and current on the inductances L and L_1 . At the same time, an increase of the radiant energy acquires a much sharper character: over the range of L from 20 to 100 nH, the radiant energy rises by a factor of 1.3–1.8 (Fig. 6, c), which agrees well with the experimental value 1.5–2.

Thus, the optimization of the laser excitation circuit with respect to the parameters of the gas-filled gap (R , L_1) and the inductance L of buses supplying current allows one to increase essentially the effectiveness of energy transfer to a discharge and the radiant energy. It's worth noting that, in the case where the energy stored in the reservoir capacitors is small (i.e. at low charging voltages), its ineffective transmission to the discharge cannot provide even the discharge ignition. The transition to the optimal values of the inductances

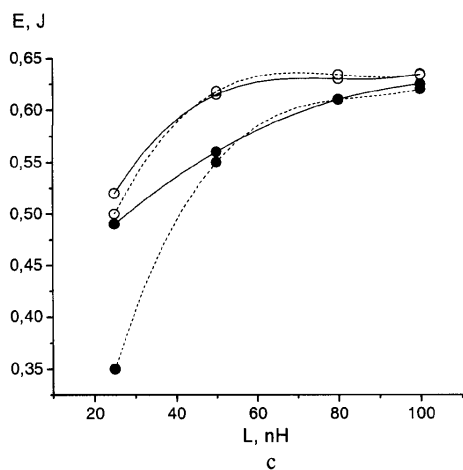
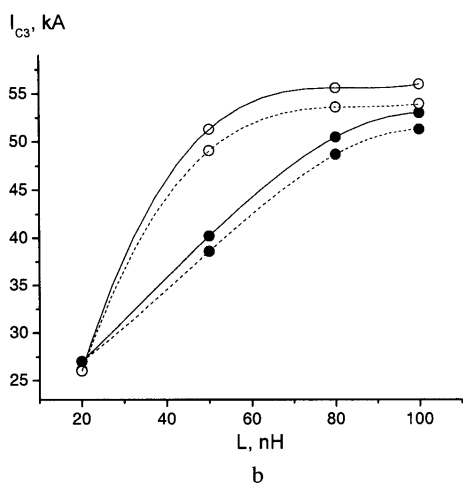
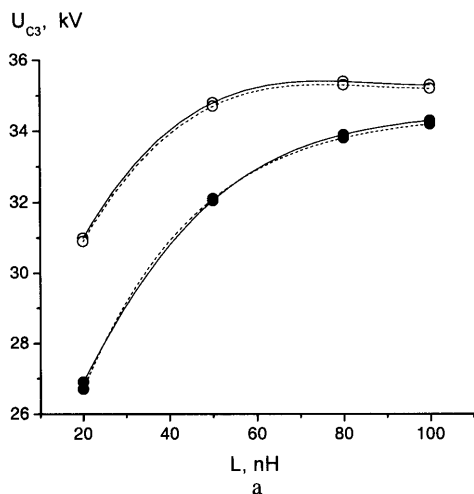


Fig. 6. Dependences of the voltage across the capacitor C_3 , current passing through it, and the radiant energy on the inductance L calculated at different values of L_1 : \bullet — $L_1=70$ nH, \circ — $L_2=40$ nH. Solid curves show the results of calculations performed for plane electrodes, dotted curves — for cylindrical ones

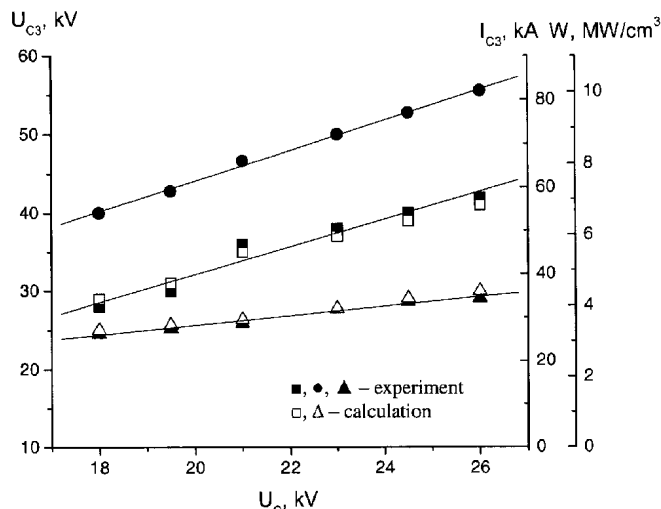


Fig. 7. Calculated and experimental dependences of the voltage across the capacitor C_3 , current passing through it, and the pumping intensity W on the charging voltage U_C . $L = 80$ nH

L and L_1 allows one to achieve the discharge burning and the generation starting from a charging voltage of 18 kV, i.e. to expand the range of working voltages towards lower values in addition to an increase of the radiant energy of a laser.

Under these conditions, by using the specially developed gas-filled gap SR and $L = 80$ nH, we obtained the dependences of the voltage across the capacitor C_3 , current passing through it, radiant energy, and total efficiency on the charging voltage varying in the range 18–26 kV. In the course of our experimental investigations, we discovered that, with increase in the charging voltage from 18 to 26 kV, the optimal pressure rises from 2.0 to 3.0 atm, discharge width from 0.6 to 1.1 cm, and, respectively, the active volume of the medium from 96 to 175 cm³. These factors were used for estimating the pumping intensity and performing the calculations which allowed us to reach a better correspondence between the results of our simulation and those of the experiments.

Figure 7 demonstrates the voltage across the capacitor C_3 , the current passing through it, and the pumping intensity W as functions of the charging voltage U_C . From the latter dependence, one can see that, with the variation in the discharge width being allowed, the pumping intensity slowly increases. At the minimal charging voltage $U_C = 18$ kV, the absolute magnitude of W amounts to 3.2 MW/cm³ while, at $U_C = 26$ kV, the value of W reaches 4 MW/cm³.

In Fig. 8, we present the results of studies of the radiant energy and the total efficiency of the KrF laser

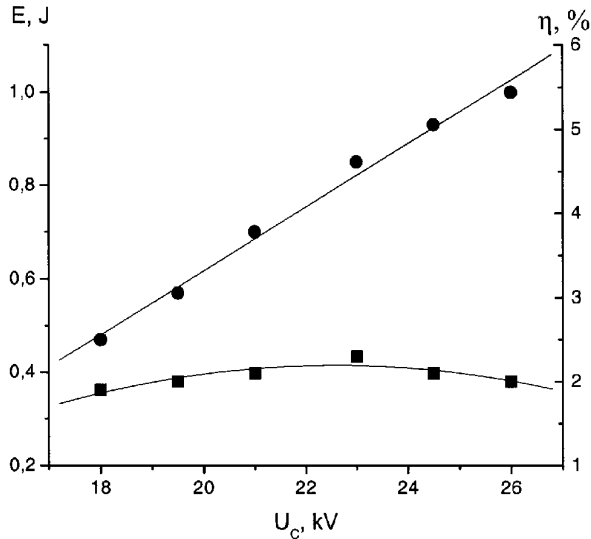


Fig. 8. Radiant energy E and the total efficiency η of a KrF laser as functions of the charging voltage measured for the active medium He—Kr—F₂ = 89.8:10:0.2. $L = 80$ nH

as functions of the charging voltage U_C . One can see that the achievement of peak values of these parameters under the given excitation conditions requires a pumping intensity of 3–4 MW/cm³, which exceeds the optimal values obtained in [1,2] when investigating a Ne—Kr—F₂ mixture laser. In the present paper, we have obtained a weak dependence of the total efficiency of a He—Kr—F₂ mixture laser on the charging voltage: the total efficiency changed from 1.9% at $U_C=18$ kV up to 2% at $U_C=26$ kV. The peak radiant energy amounted to 1 J at an efficiency of 2%.

5. Conclusions

The influence of the parameters of the excitation system and the active medium on the radiant energy and efficiency of a KrF laser is investigated experimentally and theoretically. An LC-inverter excitation circuit with a sharpening capacitor, the automatic UV preionization, and a spark gap used as a high-voltage switch is analyzed. The optimal parameters of the elements of the excitation circuit are determined, which provides the pumping intensity approximately equal to 4 MW/cm³. It is discovered that, with increase in the pumping level, there occurs a rise of both the total pressure of the active medium and the active volume due to an increase in the discharge width. The comparison of the results obtained for KrF and ArF lasers testifies to the fact that the dependences of the discharge and radiation characteristics on the parameters of the excitation circuit have a universal form.

1. Borisov V.M., Bragin I.E., Vinokhodov A.Yu., Vodchits V.A. // Kvant. Elektr. — 1995. — **22**. — P.533–536.
2. Borisov V.M., Borisov A.V., Bragin I.E. // Ibid. — P. 446–450.
3. Miyazaki K., Hasama T., Yamada K. et al. // J. Appl. Phys. — 1986. — **60**. — P. 2721–2728.
4. Armandillo E., Bonanni F., Grasso G. // Opt. Commun. — 1982. — **42**. — P.63–82.
5. Watanabe S., Endoh A. // Appl. Phys. Lett. — 1992. — **41**. — P.799–801.
6. Nodomi R., Oeda Y., Sajiki K., Nakajima S. et al. // IEEE J. Quantum Electronics. — 1991. — **27**. — P.441–444.
7. Zhupikov A.A., Razhev A.M. // Kvant. Elektr. — 1998. — **25**. — P.687–689.
8. Razhev A.M., Zhupikov A.A., Kargapoltsev E.S. // Ibid. — 2004. — **34**. — P.95–99.
9. Sutton D.G., Suchard S.N., Gibb O.L. // Appl. Phys. Lett. — 1976. — **28**. — P.522–524.
10. Razhev A.M., Shchedrin A.I., Kalyuzhnaya A.G. et al. // Kvant. Elektr. — 2004. — Vol.34, P.901–906.
11. Hsia J. // Appl. Phys. Lett. — 1977. — **30**. — P.101–106.
12. Luches A., Nassisi V., Perrone M.R. // J. Phys. E: Sci. Instrum. — 1987. — **20**. — P.1015–1018.
13. Zhupikov A.A., Razhev A.M. // Kvant. Elektr. — 1997. — **24**. — P.683–687.
14. Lo D., Shchedrin A.I., Ryabtsev A.V. // J. Appl. Phys. — 1996. — **29**. — P.43–49.
15. Baginskii V.M., Belokrivitskii N.S., Golovinskii P.M. et al. // Kvant. Elektr. — 1990. — **17**. — P.1390–1394.

Received 21.02.05.

ЗАЛЕЖНІСТЬ ЕФЕКТИВНОСТІ ЕКСИМЕРНИХ ЕЛЕКТРОРОЗРЯДНИХ ЛАЗЕРІВ ВІД ПАРАМЕТРІВ СИСТЕМИ ЗБУДЖЕННЯ І АКТИВНОГО СЕРЕДОВИЩА

О.М. Ражев, А.А. Жупіков, А.І. Щедрін, Г.Г. Калюжна

Резюме

Наведено результати теоретичних і експериментальних досліджень впливу параметрів системи збудження і активного середовища на енергію генерації і ККД KrF-лазера. Теоретично проаналізовано систему збудження типу LC-інвертор з загострювальною емністю, автоматичною УФ-передіонізацією та іскровим розрядником у ролі високовольтного комутатора. Знайдено оптимальні параметри елементів системи збудження, що забезпечують питому потужність накачки близько 4 МВт/см³. Виявлено, що із збільшенням рівня накачки відбувається збільшення оптимального тиску активного середовища, в також активного об'єму за рахунок зростання ширини розряду. Порівняння результатів, що одержані для KrF- та ArF-лазерів, свідчить про універсальний характер залежностей характеристик розряду та випромінювання від параметрів системи збудження.